Yuzuncu Yil University
Journal of the Institute of Natural & Applied Sciences

https://dergipark.org.tr/en/pub/yyufbed

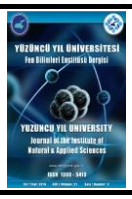

Research Article

Theoretical Investigation of the Chemical Reactivity of Acrylic Acid Molecules: A DFT Study with UV-Vis, NMR, and FT-IR Spectroscopy Using STO-3G Basis Set

Fermin AK*, Mehmet Hanifi KEBİROĞLU

Malatya Turgut Özal University, Darende Bekir Ilıcak Vocational School, Opticianry Program, 44700, Malatya, Türkiye
Fermin AK, ORCID No: 0000-0003-3238-4638,
Mehmet Hanifi KEBİROĞLU, ORCID No: 0000-0002-6764-3364
*Corresponding author e-mail: fermin.ak@ozal.edu.tr

Article Info

Received: 27.08.2023
Accepted: 25.10.2023
Online August 2024

DOI:10.53433/yyufbed.1350755

Keywords
Acrylic Acid,
FT-IR,
HOMO and LUMO,
NMR,
UV-Vis

Abstract: In this paper, quantum computational chemistry methods were employed to calculate the molecular characteristics of acrylic acid. Density Functional Theory (DFT) was used to optimize the molecule at the STO-3G basis set to calculate the highest occupied molecular orbital (HOMO) and lowest unoccupied molecular orbital (LUMO) energy levels of the frontier orbitals of acrylic acid. The energy gap between HOMO-LUMO orbitals was calculated to be 5.545 eV. This demonstrated that the energy gap reflects the chemical activity of the molecule. The compound was characterized by UV-Visible, Nuclear Magnetic Resonance (NMR), and Fourier Transform Infrared (FT-IR) spectroscopy methods.

Akrilik Asit Moleküllerinin Kimyasal Reaktivitesinin Teorik İncelenmesi: STO-3G Temel Seti Kullanılarak UV-Vis, NMR ve FT-IR Spektroskopisi ile Bir DFT Çalışması

Makale Bilgileri

Geliş: 27.08.2023
Kabul: 25.10.2023
Online Ağustos 2024

DOI:10.53433/yyufbed.1350755

Anahtar Kelimeler
Akrilik Asit,
FT-IR,
HOMO ve LUMO,
NMR,
UV-Vis

Öz: Bu yazıda, akrilik asidin moleküler özelliklerini hesaplamak için kuantum hesaplamalı kimya yöntemleri çalışılmıştır. Yoğunluk Fonksiyonel Teorisi (DFT), akrilik asidin sınır orbitallerinin en yüksek dolu moleküler orbital (HOMO) ve en düşük boş moleküler orbital (LUMO) enerji seviyelerini hesaplamak için STO-3G temel setinde molekülü optimize etmek için kullanılmıştır. HOMO-LUMO orbitalleri arasındaki enerji aralığı 5.545 eV olarak hesaplanmıştır. Bu, enerji aralığının molekülün kimyasal aktivitesini yansıttığını göstermiştir. Bileşik; UV-Görünür, Nükleer Manyetik Rezonans (NMR) ve Fourier Dönüşümü Kızılötesi (FT-IR) spektroskopi yöntemleri ile karakterize edilmiştir.

1. Introduction

Acrylic acid is frequently utilized in grafting procedures as a spacer to link proteins and the substrate. The chemical formula for Polyacrylic acid (PAA) is $C_3O_2H_4$ (Zhang et al., 2014). Furthermore, through functional analysis, a deeper comprehension of the molecular signaling pathways related to surface coating has been achieved. This understanding holds significant potential for advancements in regenerative medicine, biomaterials, and tissue engineering. Commercially available contact lenses are surface-modified using plasma polymerization (Naganandhini et al., 2022). Studies on the polymerization of acrylic acid molecules and the interactions of polyacrylic acid with various polymer blends have been extensively documented in the literature. FT-IR, FT-Raman, and FT-NIR techniques have been used for the various H– bonded structures of acrylic acid (Issaoui et al., 2017). Intermolecular hydrogen bonds play a crucial role in maintaining the stability of the molecule (Kanmazalp, 2017). Density functional theory (DFT), a quantum chemical computation approach, has been extensively employed to ascertain the molecular structure and electronic characteristics of polyatomic molecules. DFT has gained significant popularity in the fields of chemistry, physics, and materials science for understanding and predicting the behavior of complex atomic-scale systems. DFT method has employed to investigate the analysis of the title compound, with a specific focus on its ground state, which corresponds to the minimum energy state (Çiftci et al., 2020; Abdel-baset, 2023). The energy gap, also known as the difference between HOMO and LUMO energies, directly impacts the chemical reactivity and kinetic stability of the molecule (Odujole & Desai, 2020). The electronic properties of nanostructures can be changed optionally. Studies have shown that doping of different atoms or functionalization can enable them to be easily adsorbed by molecules (Bibi et al., 2021). The studies have also shown that they influence the performance of optoelectronic devices (Muz & Kurban, 2019; Muz & Kurban, 2020).

Acrylic acid was investigated by quantum chemical computation and bioactivity analysis. We reported the results of DFT computations, which is a commonly used method for studying chemical reactivity to determine chemical stability (Frau et al., 2017). NMR, FT-IR, UV-vis spectroscopy, and other parameters used as characterization techniques were also investigated in the study.

2. Material and Methods

The Gaussian 09W software package was utilized to construct and study the structure of acrylic acid molecule. Initially, two methods were chosen: DFT and HF. By choosing the basis sets of these two methods separately, the optimized states of the structure were created. As given in Table 1, we decided to use STO-3G as the best fit for the energy range of the results. DFT is employed for quantum chemical calculations at the optimized structure (Tanış, 2022a). In the literature, DFT calculations have become a valuable tool that yields highly reliable results for molecular geometry, electronic, and optical properties when compared to experimental data (Tanış, 2022b). These theoretical investigations are crucial for time and cost savings as well as for optimizing experimental procedures (Tanış, 2022c).

Table 1. The energy gap between HOMO-LUMO orbitals of sets

Sets	DFT (eV)	HF (eV)
STO-3G	5.545	15.324
3-21G	6.086	13.805
6-31G	6.026	13.397
6-31G'	6.026	13.397
6-311G	6.026	13.314
LanL2DZ	5.919	13.056
LanL2MB	5.545	15.324
SDD	5.918	13.064

After optimizing the structure using GaussView 6.0 software, NMR, UV, and FT-IR were performed (Sucheta et al., 2022). The GaussSum program was used to determine the DOS (density of states) spectrum (O'boyle et al., 2008). The vibrational wave numbers and other parameters were calculated using optimized structural parameters.

Molecular chemical reactivity and conductivity can be interpreted by the HOMO-LUMO energy gap (Parr & Yang, 1984; Diomande & Kone, 2019). A minimal energy gap indicates molecular stability and allows electrons to transition into excited states more easily. The compound with the smallest band gap is more polarized and chemically reactive. Molecular polarizability is important for optical and biological activity. The parameter formulas used for this are shown below.

$$I = -E_{HOMO} \tag{1}$$

$$A = -E_{LUMO} \tag{2}$$

$$\eta = \frac{1}{2}\left[\frac{\partial^2 E}{\partial^2 N}\right]_{v(r)} = \frac{I - A}{2} \tag{3}$$

$$\sigma = \frac{1}{\eta} \tag{4}$$

$$\mu = -\chi = \left[\frac{\partial E}{\partial N}\right]_{V(r)} = -\left(\frac{I + A}{2}\right) \tag{5}$$

$$\omega = \frac{\chi^2}{2\eta} \tag{6}$$

$$\varepsilon = \frac{1}{\omega} \tag{7}$$

$$\omega^{+} = \frac{(I + 3A)^2}{16(I - A)} \tag{8}$$

$$\omega^{-} = \frac{(3I + A)^2}{16(I - A)} \tag{9}$$

Molecular polarizability is of great importance in modeling molecular properties, optical properties, and biological activity. These equations are used to calculate ionization energy, electron affinity, chemical potential (μ), electronegativity (χ), spherical hardness (η), and softness (σ) (Çakmak et al., 2022). Table 2 shows the chemistries obtained in the gas phase at the B3LYP/STO-3G ground level. Quantum chemical parameters provide theoretical predictions that can be used to determine the activity of molecules. Figure 1 shows the energy level diagram of acrylic acid, with the HOMO and LUMO orbitals highlighted.

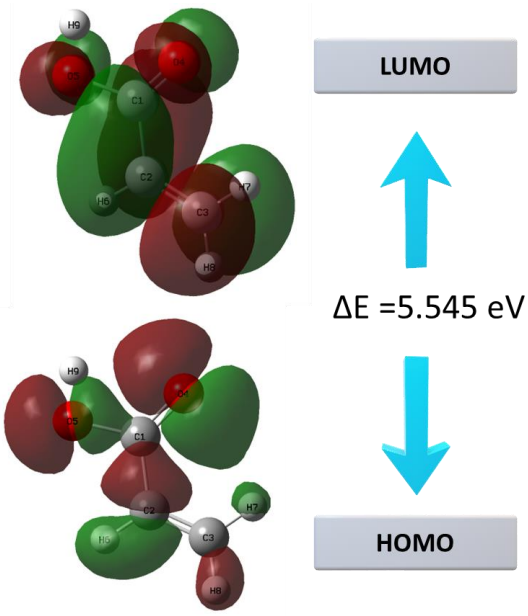

Figure 1. HOMO-LUMO structure with the energy level diagram of Acrylic Acid.

Table 2. The calculated quantum chemical descriptors for Acrylic Acid

Parameter	Values
E_{HOMO} **(eV)**	-4.191
E_{LUMO} **(eV)**	1.354
ΔE **(eV)**	5.545
η (eV)	2.772
σ (eV^{-1})	0.361
χ (eV)	1.418
μ (eV)	-1.418
ω	0.362
ε	2.762
ω^+	1.876
ω^-	1.418

3. Results

3.1. Vibrational spectroscopic analysis spectrum

When the dipole moment of the molecule changes during vibration, infrared becomes active (i.e., absorbs incoming infrared radiation) (Griffiths & de Haseth, 1986). As a result, symmetrical oscillations are rarely observed in the infrared spectrum. If a molecule has a center of symmetry, not all symmetrical vibrations around the center will be active in the infrared spectrum (Qiu et al., 2018). On the other hand, asymmetric vibrations of all molecules are detected. This lack of selectivity allows the characterization of almost all chemical groups in a single sample that is difficult to detect with conventional spectroscopic techniques (Messick et al., 2008). Among the different characterization methods, Fourier transform infrared (FT-IR) spectroscopy is one of the most powerful tools for

determining the functional group in possible molecular bonds between chemical compounds (Mohamed et al., 2015; Mohamed et al., 2016). Understanding the positions of IR absorption bands in the spectrum as wavenumbers can be used to identify various chemical compounds that are undetectable in X-ray photoelectron spectroscopy spectra. In general, IR spectroscopy is applicable to a wide variety of materials and situations and can be used for qualitative and quantitative analysis (Pavia et al., 2001). The key to understanding an FT-IR spectrum is to identify the positions, relative sizes, vibrational types, and changes in the spectrum pattern of all absorptions or peaks. This information can be used to gain valuable and informative insights (Smith, 2006; Khoshhesab, 2012).

It shows the estimated FT-IR spectra of the studied molecules in the range of 4000 cm^{-1} to 0 cm^{-1}.The frequencies in the figure are harmonic frequencies. Harmonic frequencies are calculated by multiplying the harmonic frequencies by the appropriate measurement factor for each calculation level. Similarity in complexes meant similarity in both spectrum and vibrational frequencies. According to the basic principles of vibrational spectroscopy, the vibrational frequency of a bond increases as the bond strength increases and the mass of the bond atom decreases. In Figure 2, the peak number 41 indicates the highest intensity, and the wavenumber indicates 1 208 cm^{-1}. Other permeability numbers, 83, 79, 60, 75, 57, and 77 peak numbers, have been changed at a low level. The peak number and wavelength of 60 to 79 indicate the energy range between 1 832 cm^{-1} and 3 392 cm^{-1}.

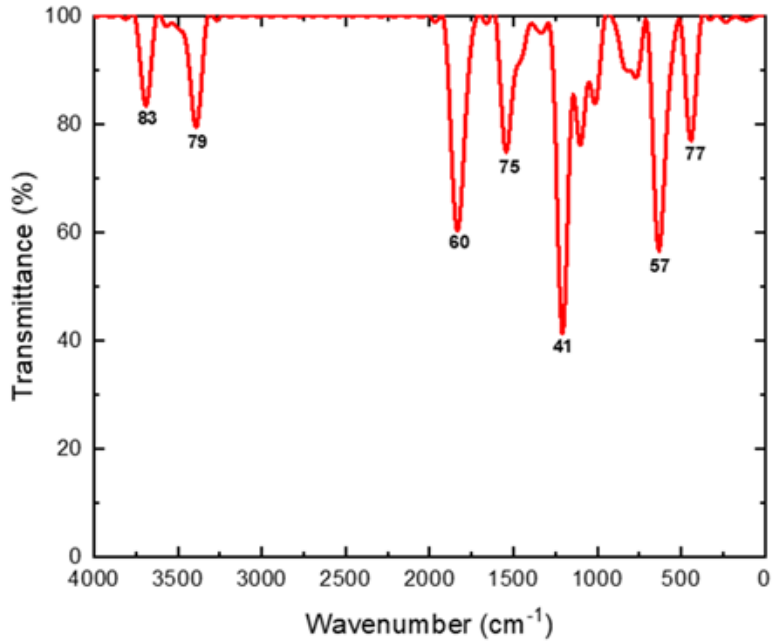

Figure 2. FT-IR spectrum of Acrylic Acid.

3.2. Nuclear magnetic resonance (NMR) investigation

Gaussian is a software package that can be used for a variety of computational chemistry tasks, including nuclear magnetic resonance (NMR) spectroscopy. It can be used to calculate NMR spectra for molecules of any size and complexity. Gaussian also includes a number of tools for analyzing NMR spectra, such as peak fitting and integration. Overall, NMR spectroscopy is an incredibly versatile tool that can be used to study a wide variety of materials, especially proteins. The rapid growth of technological advances in NMR spectroscopy has made it an essential tool for research in biochemistry, biology, and medicine (Singh & Singh, 2022).

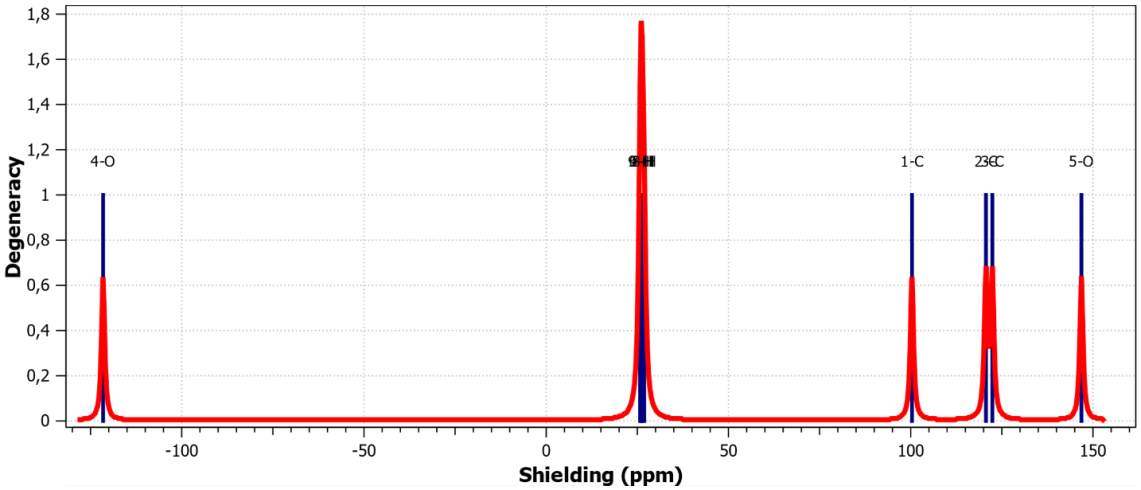

Figure 3. NMR spectrum of Acrylic Acid.

Table 3. Chemical shifts of Acrylic Acid

Method	Shielding (ppm)
4-O	-121.568
9-H	25.7572
6-H	26.0694
7-H	26.3312
8-H	26.8781
1-C	100.3448
2-C	120.6442
3-C	122.3991
5-O	146.8408

Figure 3 shows the NMR spectra of two acrylic acid molecules. The spectra are plotted as a function of the chemical shift, which is a measure of the shielding of an atom's nucleus from the external magnetic field. Table 3 lists the calculated chemical shift values for each atom in the acrylic acid molecule. These values are determined by the electronic environment of the atom, which is influenced by the atoms that are bonded to it. The sudden peaks in the graph of the NMR spectra indicate the locations of distinctive features in the acrylic acid molecule structure. These features include the carboxylic acid group, the carbon-carbon double bond, and the hydrogen atoms attached to the carbon atoms.

3.3. UV-Visible analysis

UV-Visible analysis is a type of spectroscopy that uses light in the ultraviolet (UV) and visible (Vis) ranges to study the electronic structure and properties of molecules. When a molecule absorbs light, it causes electrons to move from a lower energy level to a higher energy level. The amount of energy that is absorbed is equal to the difference in energy between the two levels. The different wavelengths of light correspond to different energies. UV light has shorter wavelengths and higher energies than visible light. The spectrum of a molecule shows the amount of light that is absorbed at each wavelength. This spectrum can be used to identify the molecule and to determine its electronic structure. UV-Visible analysis is a powerful tool for studying the properties of molecules (Schmid, 2001).

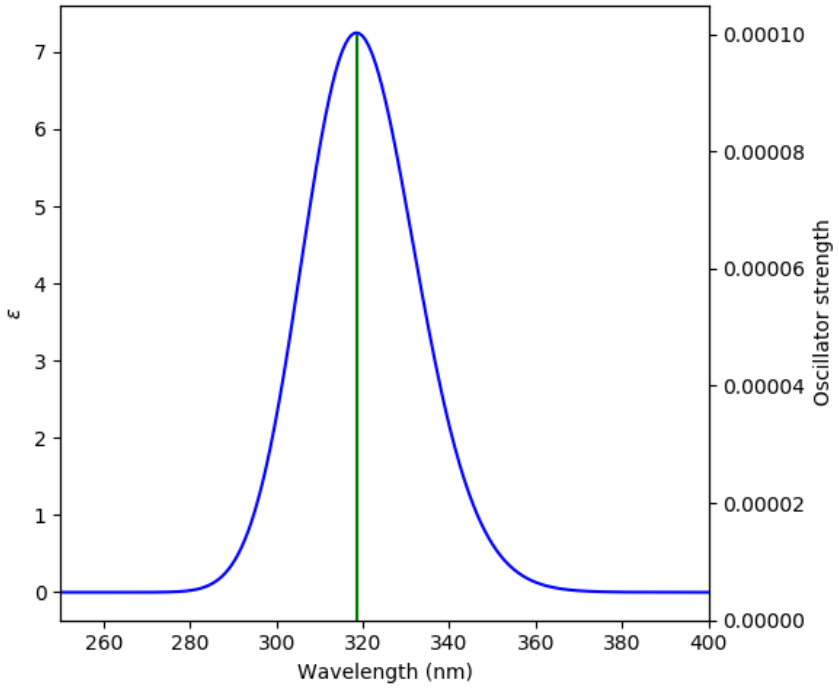

Figure 4. UV-visible absorption spectrum of Acrylic Acid.

Table 4. Peak information of Acrylic Acid

Acrylic Acid	
Wavelength (nm)	**Strength**
318.52	121.0843162
202	29181.3202
170.64	121.0843162
164.81	0
160.7	392192.1001
138.8	31845.17516

Figure 4 shows the UV-visible absorption spectra of the compound. Table 4 shows wavelength (nm) and strength values. In the case of Acrylic Acid, the UV absorption spectrum covers the wavelength range from 138.8 nm to 318.52 nm. The highest peak observed at 318.52 nm. This range has absorption, especially in conjugated systems, indicating the presence of double or triple bonds within the molecule.

4. Discussion and Conclusion

The structural, electrical, chemical, and biological actions of acrylic acid are described in this study. This molecule is crucial in the medicinal and biological industries. The reactivity of the compounds as evaluated using the STO-3G basis set in a DFT calculation. It can also categorize substances appropriately based on their reactivity. Biochemical and biological activity changes are quite apparent. When using FT-IR, peak 41 represents the maximum intensity, and the wavelength is 1208 cm^{-1}. Other peak permeability numbers, including 83, 79, 60, 75, 57, and 77, have been changed at a low level. It denotes the energy range between peak numbers 60 and 79. The absorbance spectra is examined using UV-visible spectroscopy. This absorption is visible and occurs in this region, the 318.52

nm peak indicates the color of the structure. The 318.52 nm peak has an energy of 5.545 eV. NMR spectra of the compound was also determined.

As a result, acrylic acid is structurally utilized in the manufacture of numerous products, including plastics, coatings, adhesives, paint, and varnish. It broadens the chemical structure detection range and is suitable for a variety of applications.

References

Abdel-baset, H. M. (2023). Electronic structure and stability of a pure sodium alanate clusters Na12Al12H48, and the interstitial space-doped with Ti, C and H atoms, as a promising hydrogen storage system: Density functional theory. *International Journal of Hydrogen Energy*, 48(53), 20430-20440. https://doi.org/10.1016/j.ijhydene.2023.03.023

Bibi, S., Urrehman, S., Khalid,L., Yaseen, M., Khan, A. Q., & Jia, R. (2021). Metal doped fullerene complexes as promising drug delivery materials against COVID-19. *Chemical Papers*, 75, 6487-6497. https://doi.org/10.1007/s11696-021-01815-4

Çakmak, R., Başaran, E., Kaya, S., & Erkan, S. (2022). Synthesis, spectral characterization, chemical reactivity and anticancer behaviors of some novel hydrazone derivatives: Experimental and theoretical insights. *Journal of Molecular Structure*, 1253, 132224. https://doi.org/10.1016/j.molstruc.2021.132224

Çiftci, E., Ata, A. Ç., Yıldıko, Ü., & Çakmak, İ. (2020). Spectroscopic comparison of 4-Isopropyl-N, N-Bis (4-Azidophenyl) Aniline molecule (IPAPA): DFT and MEP Analysis. *Journal of the Institute of Science and Technology*, 10(3), 1799-1810. https://doi.org/10.21597/jist.687723

Diomande, S., & Kone, S. (2019). Lipophilicity and QSAR study of a series of makaluvamines by the method of the density functional theory: B3LYP/6-311++G(d,p). *Journal of Materials Physics and Chemistry*, 7(1), 20-28.

Frau, J., Muñoz, F., & Glossman-Mitnik, D. (2017). Application of DFT concepts to the study of the chemical reactivity of some resveratrol derivatives through the assessment of the validity of the "Koopmans in DFT" (KID) procedure. *Journal of Theoretical and Computational Chemistry*, 16 (01), 1750006. https://doi.org/10.1142/S0219633617500067

Griffiths, P. R., & de Haseth, J. A. (1986). *Fourier Transform Infrared Spectroscopy, Vol. 83 aus der Reihe: Chemical Analysis—A Series of Monographs of Analytical Chemistry and Its Applications.* John Wiley Sons. https://doi.org/10.1002/bbpc.19860901224

Issaoui, N., Ghalla, H., Bardak, F., Karabacak, M., Dlala, N. A., Flakus, H. T., & Oujia, B. (2017). Combined experimental and theoretical studies on the molecular structures, spectroscopy, and inhibitor activity of 3-(2-thienyl) acrylic acid through AIM, NBO, FT-IR, FT-Raman, UV and HOMO-LUMO analyses, and molecular docking. *Journal of Molecular Structure*, 1130, 659-668. https://doi.org/10.1016/j.molstruc.2016.11.019

Kanmazalp, S. D. (2017). Investigation of theoretical calculations of 2-(1-Phenylethylideneamino) guanidine compound: NBO, NLO, HOMO-LUMO and MEP analysis by DFT Method. *Karaelmas Science and Engineering Journal*, 7(2), 491-496.

Khoshhesab, Z. M. (2012). Reflectance IR Spectroscopy. In: T. Theophanides (Ed.), *Infrared Spectroscopy - Materials Science, Engineering and Technology,* (pp. 233e44). InTech. https://doi.org/10.5772/37180

Messick, T. E., Russell, N. S., Iwata, A. J., Sarachan, K. L., Shiekhattar, R., Shanks, J. R., ..., & Marmorstein, R. (2008). Structural basis for ubiquitin recognition by the Otu1 ovarian tumor domain protein. *Journal of Biological Chemistry*, 283(16), 11038-11049. https://doi.org/10.1074/jbc.M704398200

Mohamed, M. A., Salleh, W. N. W., Jaafar, J., Ismail, A. F., Abd. Mutalib, M., & Jamil, S. M. (2015). Feasibility of recycled newspaper as cellulose source for regenerated cellulose membrane fabrication. *Journal of Applied Polymer Science*, 132, (43). https://doi.org/10.1002/app.42684

Mohamed, M. A., Salleh, W. N. W., Jaafar, J., Hir, Z. A. M., Rosmi, M. S., Mutalib, M. A., ..., & Tanemura, M. (2016). Regenerated cellulose membrane as bio-template for in-situ growth of visible-light driven C-modified mesoporous titania. *Carbohydrate Polymers*, 146, 166-173. https://doi.org/10.1016/j.carbpol.2016.03.050

Muz, İ., & Kurban, M. (2019). Enhancement of electronic, photophysical and optical properties of 5,5' -Dibromo-2,2' -bithiophene molecule: new aspect to molecular design. *Opto-Electronics Review*, 27, 113-118. https://doi.org/10.1016/j.opelre.2019.03.002

Muz, İ., & Kurban, M. (2020). Electronic transport and non-linear optical properties of hexathiopentacene (HTP) nanorings: A DFT study. *Journal of Electronıc Materials*, 49(5), 3282-3289. https://doi.org/10.1007/s11664-020-08017-w

Naganandhini, S. P., Sangeetha, T., Sahana, R., Mounica, P., Rajmohan, G., Dineshkumar, P., & Arivazhagan, G. (2022). Theoretical discussion on the hydrogen bond ınteractions between Acrylic Acid dimer and dibutyl ether Monomer. *Computational and Theoretical Chemistry*, 1213, 113746. https://doi.org/10.1016/j.comptc.2022.113746

O'boyle, N. M., Tenderholt, A. L., & Langner, K. M. (2008). Cclib: a library for package-independent computational chemistry algorithms. *Journal of Computational Chemistry*, 29(5), 839-845. https://doi.org/10.1002/jcc.20823

Odujole, J. I., & Desai, S. (2020). Molecular dynamics simulations of PAA as resist for nanoimprint lithography. In L. Cromarty, R. Shirwaiker, P. Wang (Eds.), *Proceedings of the 2020 IIE Annual Conference* (pp. 221-226). Institute of Industrial and Systems Engineers (IISE).

Parr, R. G., & Yang, W. J. (1984). Density functional approach to the frontier-electron theory of chemical reactivity. *Journal of the American Chemical Society*, 106, 511-516. https://doi.org/10.1021/ja00326a036

Pavia, D. L., Lampman G. M., & Kriz, G.S. (2001). *Introduction to Spectroscopy*. 3rd ed. USA: Thomson Learning, Inc.

Qiu, L., Levine, K., Gajiwala, K. S., Cronin, C. N., Nagata, A., Johnson, E., ... & Sun, S. (2018). Small molecule inhibitors reveal PTK6 kinase is not an oncogenic driver in breast cancers. *PLoS One*, 13(6), e0198374. https://doi.org/10.1371/journal.pone.0198374

Schmid, F. X. (2001). Biological Macromolecules: UV-visible Spectrophotometry. In *Encyclopedia of Life Sciences.* https://doi.org/10.1038/npg.els.0003142

Singh, M. K., & Singh, A. (2022). Chapter 14 - Nuclear magnetic resonance spectroscopy. In M. K. Singh & A. Singh (Eds.), *Characterization of Polymers and Fibres* (pp. 321–339). Woodhead Publishing. https://doi.org/10.1016/B978-0-12-823986-5.00011-7

Smith, B. (2006). *Fundamentals of Fourier Transform Infrared Spectroscopy.* USA: CRC Press Taylor & Francis Group.

Sucheta, M., Pramod, A. G., Zikriya, M., Salma, K. M., Venugopal, N., Chaithra, R., ..., & Murthy, S. (2022). Frontier molecular orbital, molecular structure and Thermal properties of 2, 4, 6, 8-tetramethyl-2, 3, 6, 7-tetrahydro-s-indacene-1, 5-dione using DFT calculation. *Materials Today: Proceedings*, 62, 5241-5244. https://doi.org/10.1016/j.matpr.2022.03.215

Tanış, E. (2022a). Study of electronic, optoelectronic and photonic properties of NBB material in solvent environments. *Journal of Electronic Materials*, 51, 4978-4985. https://doi.org/10.1007/s11664-022-09730-4

Tanış, E. (2022b). New optoelectronic material based on biguanide for orange and yellow organic light emitting diode: A combined experimental and theoretical study. *Journal of Molecular Liquids*, 358, 119161. https://doi.org/10.1016/j.molliq.2022.119161

Tanış, E. (2022c). A study of silicon and germanium-based molecules in terms of solar cell devices performance. *Turkish Journal of Chemistry*, 46, 1607-1619. https://doi.org/10.55730/1300-0527.3464

Zhang, H., Brown, K. D., Lowe, S. P., Liu, G. S., Steele, D., Abberton, K., & Daniell, M. (2014). Acrylic acid surface-modified contact lens for the culture of limbal stem cells. *Tissue Engineering Part A*, 20(11-12), 1593-1602. https://doi.org/10.1089/ten.tea.2013.0320